JOURNAL OF MATERIALS SCIENCES 33 (1998) 1887–1895

Microstructures and leach rates of glass–ceramic nuclear waste forms developed by partial vitrification in a hot isostatic press

S. V. RAMAN
Nuclear Engineering Department, Idaho National Engineering and Environmental Laboratory, Lockheed Martin Idaho Technologies, Idaho Falls, ID 83402, USA
E-mail: ramasv@inel.gov

A high level nuclear waste calcine simulant is transformed to a dense and durable glass–ceramic waste form by addition of glass and crystal forming components, and hot isostatic pressing at 1000 °C and 138 MPa. The waste forms are abundantly composed of zircon, beddeyelite, apatite, fluorite, greenockite and boroaluminosilicate glass. The crystal nucleating, glass forming and volatilizing components of the calcine are partitioned into crystalline and glass phases such that 95 wt% of the waste components, including actinide surrogates, stoichiometrically reside in the crystalline phases. This results in a high waste loading of 60–80 wt% calcine in the total glass–ceramic. The partitioning follows the natural association of elements, as a result, species like P avoid the glass phase. Instead glass accommodates the incompatible solutes like Cs. It minimizes porosity and bonds the polyphase ceramic microstructure, which resembles rhyolite or basalt volcanic rocks. Both glass and crystals contribute to high chemical durability, which is degraded when glass devitrifies with lowering of partial liquid viscosity by higher MgO additions. The devitrified phases are layered mica, dendritic nepheline and fibrous alkaline-earth borate. These phases are enriched in the mobile elements of Cs, Na and B, respectively. © *1998 Chapman & Hall*

1. Introduction

The processing feasibility has inclined much of the scientific endeavour towards developing borosilicate glass varieties for immobilizing waste solutes. Yet concerns have surfaced on its long range durability and its limited application to a variety of waste streams. As an alternate, crystalline materials that are compositionally and structurally compatible with durable ceramic and mineral matter have been in parallel development [1–14]. The recent surge for developing processes to grow crystalline phases stems from the efforts to disposition the excess weapons grade plutonium [15–18]. Problems still remain regarding durable long range immobilization, because many high level nuclear wastes contain besides fission products and actinides, components that are related to spent fuel dissolution technology. The waste characteristics are nuclear processing plant specific, and hence entail treatment variations for their transformation to suitable waste forms [4, 14, 19–21]. For example, the fuel cladding, hydrofluoric acid dissolution, and dolomite bed calcination of the waste liquid resulting from U-235 and Kr-85 separations compose the complex calcined wastes of the Idaho Chemical Processing Plant (ICPP), that is of interest in this paper.

Higher concentrations of nucleating agents coupled with the presence of volatiles complicate vitrification of some of the high level ICPP wastes into homogeneous glass [22–24]. The calcine contains transuranics; fission products, Cs and Sr; transition elements; and volatiles, Cl and S in minor to trace amounts. The major components of the calcine are Al_2O_3, B_2O_3, ZrO_2, CaF_2, Na_2O, CaO and CdO. The main task in the immobilization is one of durably accommodating the major components in a variety of crystalline and glass phases that are also acceptors of transition elements, fissile elements, fission products and volatile traces. In order to design a technologically promising process, it is necessary to understand how the waste elements spontaneously partition among a variety of phases. The natural distribution of elements, as described by the pioneering geochemical classification of Goldschmidt, and the chemical bonding rules provide the initial basis for adding crystal and glass forming species to transform the multicomponent calcined wastes into durable waste forms [4, 22]. A series of experiments in the hot isostatic press were undertaken to:

1. evaluate the consistency between predicted phases on the basis of natural association of elements and their actual experimental development,

2. determine the distribution of waste components among glass and natural crystalline analogues to address waste loading and durability, and

3. assess the role of liquid viscosity in the development of durable microstructures.

2. Experimental procedure

2.1. Formulation of glass–ceramic composition

A typical simulated calcine composition of ICPP is shown in Table I. The liquid waste is transformed to granular calcine in an oxidizing environment of the pilot plant calciner [4]. Cerium was introduced in the calcine as surrogate for actinides. The radioactive fission products were replaced by stable isotopes of Sr and Cs. The additives are shown in Table II. They were selected such that the calcine could be transformed into a set of mineral assemblages and glass. Thus, the calcine is substantiated by Al and Si metal reductants, glass former SiO_2, glass modifier MgO and nucleating agent P_2O_5. The mass fractions among calcine and additive components were determined on the basis of crystalline phase stoichiometry and relative abundances. The major components of the calcine are partitioned among the potential crystals, such as baddeyelite, zircon, fluorite, nepheline, albite, anorthite, apatite, greenockite and cadmium metal, and boroaluminosilicate glass. The minor and trace components supposedly will occur as interstitial and atomic substituents in glass and crystalline matter.

TABLE I Calcine composition (wt% oxides)

Oxides	Wt%
B_2O_3	2.90
Al_2O_3	9.60
CrO_2	1.20
CaF_2	39.40
CaO	12.20
CdO	5.70
Ce_2O_3	1.20
Cs_2O	0.50
K_2O	1.10
MgO	0.50
Na_2O	5.10
P_2O_5	0.50
SrO	0.60
Cl^-	0.10
SO_4^{2-}	2.60
ZrO_2	17.50

2.2. Waste canister preparation

The calcine and additives were mechanically blended and packed into prototype stainless steel cylinders under a load of 2268 kg. The cylinders on average were 76 mm high, 25 mm in diameter and 0.9 mm thick. They were compacted with 60 g of calcine additive batch powder and vacuum welded.

2.3. Hot isostatic pressing (HIP)

The waste canisters were hot isostatically pressed at 138 MPa and 1000 °C using an Autoclave Engineers Inc. HIP. Pressure and temperature were monitored by transducer and R-type thermocouple. The sample chamber was pressurized using argon gas and four samples were HIPed per experiment. Because the pressure and temperature can be independently varied in the HIP, the experimental cycle consisted of first increasing the pressure to 100 MPa; second increasing the temperature to 1000 °C at 10 °C min^{-1} with concomitant rise in pressure to 138 MPa; and third isothermal treatment of 1000 °C for 4 h, which was followed by ambient cooling.

2.4. Microstructure characterization

The HIPed waste forms were examined in the X-ray powder diffractometer, polarizing optical microscope with differential interference contrast prisms, and electron microprobe for phase abundances, phase composition and intergranular relations. Standard laboratory procedures were adopted for analysing the powders and polished thin sections. Quantitative wave length dispersive electron microprobe analysis of glass and crystalline phases were obtained using suitable mineral and glass standards in the Jeol 8900 superprobe.

2.5. Leaching tests

MCC-1 test procedures were followed for leach testing waste form monoliths in the deionized water at 90 °C [25, 26]. The monoliths were cut from the centre of the cylindrical waste form as cubic or rectangular blocks. Their surfaces were polished and geometric surface areas were measured using vernier calipers. The leachant–sample ratio was maintained at 10 : 1. The

TABLE II Formulation of additive compositions

Calcine	+	Additives	→	Components in the waste form
O	+	Al/Si	→	Al_2O_3/SiO_2
All components	+	$MgO + SiO_2$	→	Boroaluminosilicate glass
ZrO_2			→	ZrO_2 (beddeyelite)
ZrO_2	+	SiO_2	→	$ZrSiO_4$ (zircon)
CaF_2			→	CaF_2 (fluorite)
Na_2O	+	$Al_2O_3 + SiO_2$	→	$NaAlSiO_4/NaAlSi_3O_8$ (nepheline/albite)
CaO	+	$Al_2O_3 + SiO_2$	→	$CaAl_2Si_2O_8$ (anorthite)
$CaO + CaF_2$	+	P_2O_5	→	$Ca_5(PO_4)_3F$ (apatite)
$CdO + SO_4$	+	Al/Si	→	$Cds/Cd + Al_2O_3/SiO_2$ (greenockite/metal)
Cl, Cr, Cs, Ce, Fe, K, Sr			→	Substituents

samples were contained in tightly covered polyethylene vials. Following 14 days of static residence time at 90 °C, the monolith was removed from the leachant. The remaining leachate liquid was acidified with dilute nitric acid in its original container and subjected to atomic absorption and induction coupled plasma spectroscopy for quantitative elemental analysis. The normalized elemental leach rates were calculated as [25, 26]

$$L_i = M_i/(A_s \times t \times F_i)$$

where, L_i is the leach rate of element i (g m^{-2} per day), M_i is the mass of element i in the leachate (g), A_s is the surface area of the monolith (m^2), t is the leaching experiment time (days), and F_i is the mass fraction of element i in the original monolith.

3. Results

3.1. Waste form composition and phase abundances

A typical bulk composition for the waste form is shown in Table III. It has resulted from the semi-empirical formulation that was intended for developing minerals and glass (Table II). The calcine–additive proportions are on the order of 1 : 1/4 by weight. Consequently, the total composition of the waste form is dominated by calcium fluoride (29.25 wt %) and zirconia (14.17 wt %). The changes to this composition were introduced by substitution of magnesia for silica and also by varying the waste loading in the 60–80 wt % range. These component exchanges cause variations in phase composition, microstructure and durability. At the same waste loading of 75 wt % the changes in phase abundance result from magnesia–silica exchange and are evident in Table IV. Beddeyelite and calcia stabilized zirconia abundances increase at the expense of zircon with decreases in silica. Concurrently, magnesium enriched phases, like mica and alkaline-earth borate, become abundant. The formation of apatite is noted in response to phosphorous addition. The cadmium oxide and sulphate components of the calcine transform to greenockite in the presence of redox additives, 2 wt % Si and 1 wt % Al. Some phases that could not be identified, and the minor phases like chromia, nepeheline, mica and cadmium metal compose the miscellaneous part of the phase composition. There is a near absence of glass with increase in magnesia at the expense of silica, which otherwise composes 23.39 wt % of the waste form (Table IV).

TABLE III Waste form compositions (wt%)

Oxides	wt%
Al_2O_3	6.49
B_2O_3	2.17
CaO	8.85
Ce_2O_3	0.90
CdO	3.00
CrO_2	0.90
Cs_2O	0.37
K_2O	0.82
MgO	1.18–6.90
Na_2O	3.67
P_2O_5	5.15
SiO_2	22.42–16.70
SrO	0.45
ZrO_2	14.17
CaF_2	29.25
Total	100.00

3.2. Microstructure

As observed in Fig. 1 the microstructure increases in grain size with decrease in calcine loading from 80–60 wt %. At high waste loadings some refractory components of the calcine, like zirconia and calcium fluoride clusters, escape reaction with additives and exist as relic features (Fig. 1). However, the relics are resorbed into glass and crystalline phases as the waste loading is decreased to 60 wt % (Fig. 1d). At 80 wt % loading, the overall granular relations are similar to that of the naturally occurring volcanic rock rhyolite, although, the two materials are distinctly different in composition (Fig. 2a and b) [27]. When the loading is reduced to 60 wt % the grains become larger and the microstructure commences to resemble the natural basalt with compositional differences (Fig. 2c and d) [27]. An average density for the waste form is on the order of 3.2 g cm^{-3}. The waste form is more than 95% dense. Some pores are present in glass and between grains. At the same waste loading, like 75 wt %, when magnesia is substituted for silica, the grains grow to larger sizes. The effect of MgO variation from 0 to 1 wt % is noted for fluorite (CaF_2), zirconia (ZrO_2) and greenockite (CdS) growths in Fig. 3a and b. Additional anomalous growth of greenockite occurs when the reducing agent Si is increased to 6 wt % and the viscosity modifier MgO is substituted for SiO_2 in the ratio of 6.9–16.70 wt % (Table III). In the same direction, increase in the transformation of CdS–Cd metal is observed in Fig. 3c. When MgO is increased at the expense of silica, other changes include the appearance of devitrified dendrites and fibres in the glass matrix. At higher proportions, like 6.9 wt % MgO, 16.7 wt % SiO_2 and 75 wt % calcine (Table III) the glass is totally devitrified into Ca–Mg borate, Mg–mica and nepheline (Fig. 3d).

3.3. Phase compositions and waste element partitioning

The results of wavelength dispersive electron microprobe analysis of predominant phases are shown in Table V. Oxygen contents for these elements were stoichiometrically calculated on the basis of the probable valence states for the cations and a divalent oxygen anion. The composition of glass, in addition to containing nearly all the elements of the calcine, is predominated by high alumina and silica (Table V). The zircon grains depart from the typical stoichiometry of $ZrSiO_4$ by the inclusion of B, Ca, Ce and Cr (Table V). Some boron is also present in apatite [$Ca_5(PO_4)_3F$] Table V]. Other important calcine elments in this mineral analogue are Ca, P, Cd, Ce

TABLE IV Phase abundance of waste forms as a function of MgO and SiO_2 variations (wt%)

Phase type	Phase abundance for MgO = 1.18 and SiO_2 = 22.42 wt%	Phase abundance for MgO = 6.90 and SiO_2 = 16.70 wt%
Fluorite, CaF_2	19.49	17.98
Beddeyelite, ZrO_2	6.82	7.06
Calcia stabilized zirconia, $Ca_{0.15}Zr_{0.85}O_{1.85}$	0.97	1.61
Apatite, $Ca_5(PO_4)_3(F, Cl)$	10.14	8.67
Zircon, $ZrSiO_4$	3.12	0.00
Greenockite, CdS	2.34	1.93
Albite–anorthite, $NaAlSi_3O_8$–$CaAl_2Si_2O_8$	5.85	0.00
Quartz, SiO_2	2.73	0.00
Ca–Mg borate	6.63	15.60
Glass	23.39	–
Calcine relic	15.59	15.59
Miscellaneous[a]	2.93	30.00
Total	100.00	98.44

[a] Miscellaneous = chromia + nepheline + alkali–earth borate + metallic cadmium + unidentified particles.

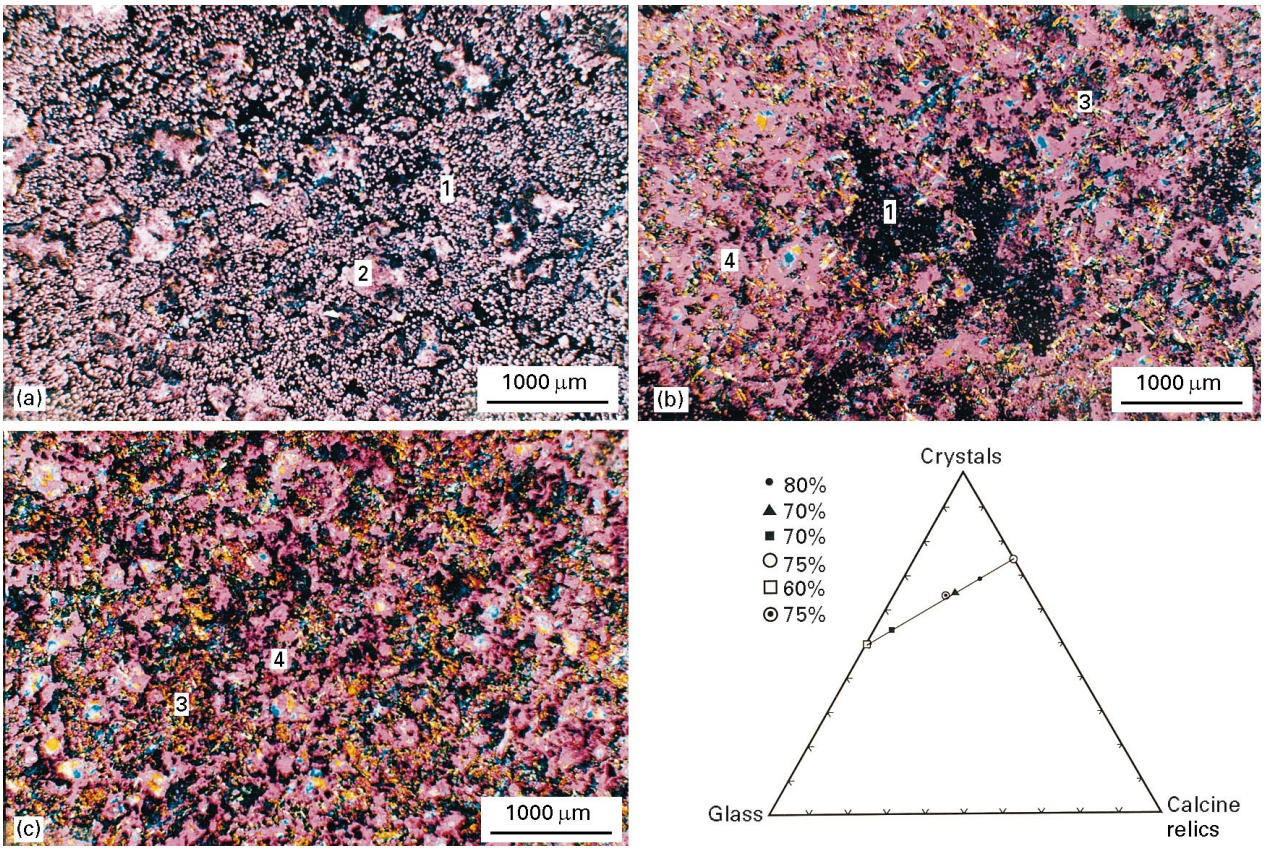

Figure 1 Transmitted light differential interference contrast micrographs of glass-ceramic waste forms with calcine loadings of (a) 80 wt %, (b) 70 wt % and (c) 60 wt %. (d) Relative weight proportions of glass, crystals and calcine relics in the waste forms (●) 80%, (▲ 70%, (■) 70%, (○) 75%, (□) 60%, (⊙) 75%. (1) spherical fluorite + zirconia grains + calcine relics, (2) glass islands, (3) acicular zircon grains, (4) fluorite + glass.

and Sr. High alumina, alkali and silica (Table V) are characteristic of nepheline. Similarly, the mineral analogue biotite is identified by its crystalline habit, and the magnesia, silica and alumina enriched chemical composition (Table V). Cs is more abundant in biotite than in other phases, including glass. The anomalous enrichment of B, Ca and Mg is representative of the alkaline-earth borate mineral suanite, that was also revealed in the X-ray powder diffraction. Departure from pure stoichiometry of $CaMgB_2O_5$ for this phase is introduced by the reasonable amounts of CeO, Na_2O and SiO_2. Fluorite (CaF_2) is the most dominant fluorine bearing phase. As noted in Table V, this mineral analogue also contains B, and calcium substituents of Cd, Ce and Sr.

Departures from compositions represented in Table V were noted, particularly for apatite and fluorite as a function of variations in metal reductant Si,

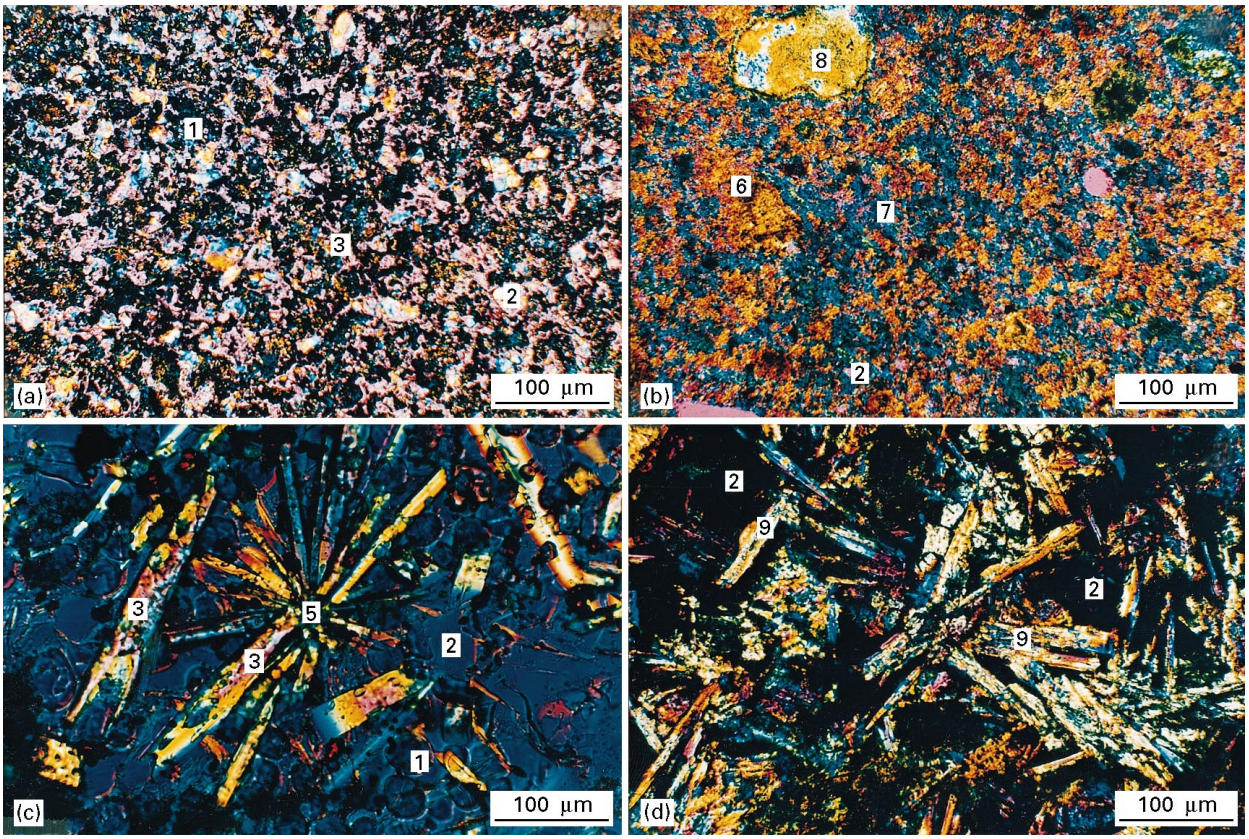

Figure 2 Microstructures of waste forms and natural rocks: (a) 80 wt % calcine loaded waste form, (b) natural rhyolite, (c) 60 wt % calcine loaded waste form, and (d) natural basalt. At 80 wt % calcine loading the waste form granularity is similar to the highly viscous volcanic rock, rhyolite. The waste form phases are (1) fluorite, (2) glass, (5) zirconia; the rhyolite phases are (6) quartz, (7) felspar, (8) inclusions, (2) glass. At 60 wt % calcine loading, the waste form microstructure resembles that of the less viscous volcanic rock, basalt. In basalt, the glass matrix (2) contains large grains of the mineral plagioclase (9). In the 60 wt % calcine waste form, the equivalent microstructure is made of large laths and crystals of zircon (3) radiating from the central zirconia particles (5) in glass (2).

magnesia–silica substitution and waste loading. Fig. 4 shows a more pronounced Ce–Ca spread for apatite than fluorite. It is also striking to note that the Sr content in both fluorite and apatite is nearly the same and is relatively insensitive to changes introduced in the waste form compositions. Table V also shows a higher concentration of Cd in apatite than fluorite. But, the bulk of Cd is partitioned into greenockite and native cadmium metal. Energy dispersive qualitative microprobe analysis reveals the association of Ce with Cd, with increases in the metal reductant.

3.4. Leachate analysis and leach rates

The 14 day MCC-1 leaching characteristics of the bulk waste forms containing $MgO–SiO_2$ weight proportions of 1.18–22.42 and 6.90–16.70 are shown in Table VI. The elemental release and, accordingly, the leach rates seem to increase significantly with magnesia for silica in the waste form. This is evident from the leach rates in the right-hand column of Na, B and Cs. Their leach rates change from 0.6 to 36.68, 0.4 to 18.78 and 0.80 to 8.37 g m^{-2} per day. However, among the elements show in Table VI, the leach rates for Zr, P, Cd and Cr are the lowest and are not significantly affected by changes in magnesia–silica substitution. Variations in the metal reductant Si from 1 to 6 wt % and waste loadings from 60 to 80 wt % also do not appear to depart the leach rates significantly for waste forms with 1.18–22.42 weight proportions of $MgO–SiO_2$ (Table VI).

4. Discussion

4.1. The role of liquid phase and volatiles

The growth of crystals and formation of high temperature compositions is favoured in these waste forms by the partial liquid phase and volatiles. The liquid phase is present in the waste form as glass, whose abundance is of the order of 23 wt % (Table IV). The glass is high in alumina and silica. Despite the presence of modifying oxides (Table V), its formation under ambient conditions requires a processing temperature of the order of 1600 °C. In the hot isostatic press the liquid phase is developed at a temperature of 1000 °C and contains the volatiles of Cs, Na, B, S, Cl and F (Table V, glass). The hot isostatic pressing process not only prevents volatile waste release to the atmosphere, but it effectively uses the latter phase in the significant depression of liquidus temperatures and formation of durable high temperature phases. Considerable porosity is eliminated by volatile solubility and liquid mobility. The movement of liquid and crystals is a spontaneous phenomenon in the hot isostatic press and is promoted by a decrease in liquid viscosity.

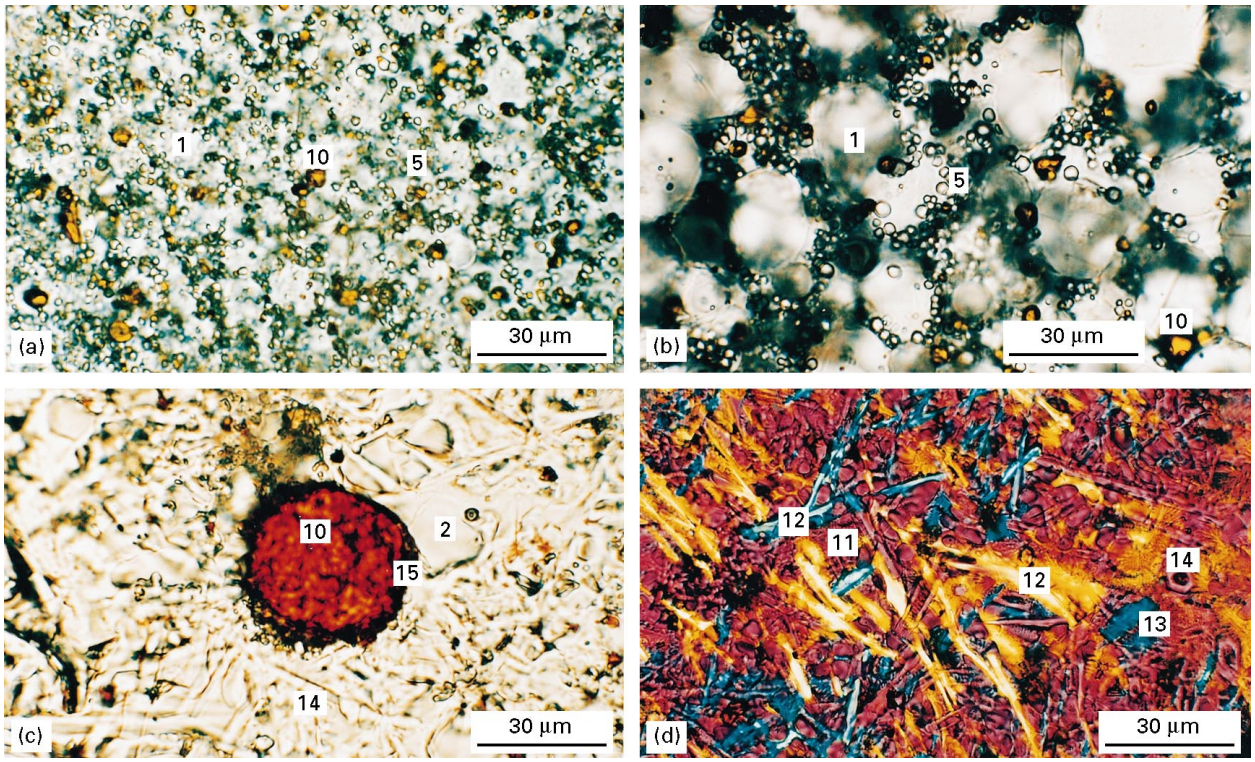

Figure 3 Grain growth as a function of MgO and Si additions: (a) 0 wt % MgO, 2 wt % Si, 1 wt % Al; (b) 1 wt % MgO, 2 wt % Si, 1 wt % Al; (c) 6.9 wt % MgO, 6 wt % Si, 1 wt % Al; (d) 6.9 wt % MgO, 2 wt % Si, 1 wt % Al. Fig. 3a–c shows increases in the growth of fluorite (1), zirconia (5) and greenockite (10). Fig. 3d shows the formation of devitrified phases of nepheline dendrites (11), alkaline-earth borates fibres (12) and mica platelets (13) in the original glass island. (14) apatite, (15) metallic cadmium.

TABLE V Representative compositions of glass and crystalline phases in the waste forms (wt %)

Oxide	Glass	Zircon	Apatite	Nepheline	Biotite	Suanite	Fluorite
Al_2O_3	19.73			35.60	17.35	2.91	
B_2O_3	3.16	0.42	0.93		1.32	32.00	B 0.24
CaO	3.17	0.39	46.86	1.67	2.64	26.30	Ca 52.18
CeO	1.02	0.49	2.24	0.07	0.31	2.23	Ce 0.27
CdO			5.93				Cd 0.11
Cr_2O_3	0.20	1.64				0.12	
Cs_2O	0.29			0.14	0.73	0.17	
K_2O	0.35			0.38	2.51		
MgO	2.06			0.17	28.40	17.89	Mg 0.11
Na_2O	1.08			15.11	2.05	8.37	Na 0.25
P_2O_5	0.20		38.15		0.34		
SiO_2	55.18	32.01		46.75	42.40	9.67	
SrO	0.53	0.12	1.04		0.44	0.19	Sr 0.48
ZrO_2	2.92	65.30					
CaF_2	8.32				1.38	0.15	
S	0.16						
Cl	0.35						
F	4.05		4.27				F 47.20

Large deformation and rupture of the waste canister under pressure of 138 MPa is prevented by maintaining a high crystal–liquid ratio. The crystal abundance is of the order of 60–80%, which is essentially the total waste loading (Fig. 1). Consequently, the microstructure is made of crystal clusters and glass islands; (Figs 1 and 2). The microstructural heterogeneity is reminiscent of natural volcanic rock, like basalt or rhyolite, with differences in the flow behaviour and total compositon. High waste loading, of the order of 80 wt % forces the crystal–liquid mush to become more viscous and crystallinity to be fine grained, as in rhyolite (Fig. 2). Despite the presence of abundant CaO in the calcine, the viscosity decrease is effectively controlled by addition of MgO. The differing behaviour between these two alkaline-earths towards melt viscosity is explained by the preferential screening of CaO into crystalline phases, like calcia-stabilized zirconia, apatite and anorthite. However, suanite and biotite are the only two magnesium enriched crystalline phases that form when the magnesia content is increased at the expense of silica. A large decrease to 16.7 wt % silica for magnesia increase to 6.9 wt % (Table III) causes a significant drop in liquid viscosity. The result

is the formation of fibrous and dendritic high surface area phases, like nepheline, suanite and biotite, in areas that otherwise would have been glass islands (Fig. 3d). Moderation in MgO addition to 1 wt % and waste loadings between 60 and 75 wt% produces basalt-like microstructure with large crystalline phases (Fig. 2).

4.2. The role of metal reductants

The metal reductants Si and Al influence partitioning of Cr, Cd and Ce among phases and also control the formation of the gaseous phase. Because the calcine is in an oxidized state, pronounced leaching is noted for Cd and Cr in the absence of reducing additives. The reductant addition forces Cd to stabilize with sulphur to form greenockite. Possibly Cr is reduced to the 4 + state, as a result it stabilizes by substitution for Zr in zircon (Table V) and by formation of CrO_2 (Table IV). Although Ce was not tested for leaching, it tends to associate with Cd in the sulphide phase with increase of reductants. In the same direction the Ce content appears to decrease in apatite (Fig. 4). A nearly constant Sr content for apatite grains in samples with varying reductants, results from limited substitution for Ca and insensitivity of Sr to redox state. Because Si is a better scavenger of oxygen than Al, the above effects are more subtle with Si addition. But higher Si (6 wt %) concentrations cause vapour phase formation, make the waste form brittle, increase transformation of CdS–Cd metal (Fig. 3c) and present a potential explosion hazard in the HIP. Alternately, these effects are minimized by addition of Al, which has a lower oxidation free energy than Si [28]. Optimum levels are of the order of 1 wt % Al and 2 wt % Si for the development of stable waste forms.

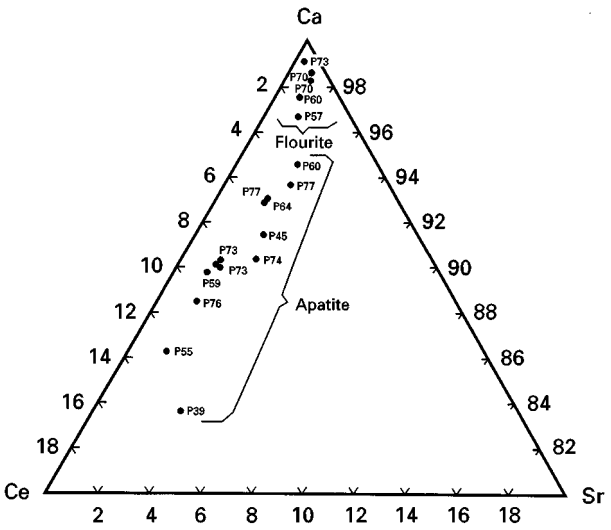

Figure 4 Relative weight proportions of Ca, Ce and Sr in apatite and fluorite.

4.3. Chemical durability

The response of glass and crystal compositions on leaching is reflected in the 14 day MCC-1 static tests. With the exception of layered, fibrous and dendritic crystals, all the other phases are more resistant to leaching. This is also characteristic of high aluminaborosilicate glass. But the crystalline phases appear more durable. This is evident from the low leach rates of the order of 0.2 g m^{-2} per day for Cd, Cr, P and Zr that preferentially concentrate in the crystals of greenockite, chromia, apatite and zircon (Table VI). Decrease in durability is imparted to the waste form by decrease in glass viscosity. The latter change is affected by increased substitution of MgO for SiO_2, and the glass is forced to devitrify during slow cooling of the waste form in the HIP. The devitrified phases have high surface areas because of their layered, fibrous and dendritic habits (Fig. 3d). They show incongruent leaching. The high release and leach rate for Na (170 μg ml^{-1}, 36.68 g m^2 per day) is attributed to its abundance in nepheline dendrites (Table VI, Fig. 3d). K and Cs are concentrated more in biotite. Their occurrence between the tetrahedral silicate layers of mica explains their mobility and enrichment in the leachate (Table VI, Fig. 3d) [29]. The high release of B (30.40 μg ml, 18.78 g m^{-2} per day) is related to its presence in the fibrous alkaline-earth borate phases (Fig. 3d, Table VI). In the absence of these phases, the leach rates of these elements are

TABLE VI Leachate analysis and leach rates

Element	For $MgO–SiO_2$ = 1.18–22.42 wt %		For $MgO–SiO_2$ = 6.90–16.70 wt %	
	Analysis (μg ml^{-1})	Rate (g m^{-2} per day)	Analysis (μg ml^{-1})	Rate (g m^{-2} per day)
Al	3.1	0.6	6.86	1.31
B	0.6	0.4	30.40	18.78
Ca	3.7	0.1	80.10	2.59
Cd	0.7	0.2	0.07	0.02
Cs	0.1	0.8	0.93	8.37
Cr	0.1	0.1	0.007	0.01
K	0.6	0.4	1.2	0.72
Mg	0.5	0.5	0.14	0.02
Na	2.8	0.6	170.0	36.68
P	0.5	0.2	0.435	0.12
Si	6.8	0.4	6.22	0.54
Sr	0.3	0.5	1.71	2.86
Zr	0.2	0.0	0.014	0.0

predominantly governed by the stability of glass. Possibly, the high alumina content accounts for high durability; as a result, the leach rates of Na, K, Cs and B are lower than 1 g m^{-2} per day, when glass is devoid of devitrification in the waste form of bulk composition shown in Table I. The low release of boron in this waste form is also attributed to its stable occupancy in crystalline lattices of zircon, apatite and fluorite (Table V). These phases in their natural mineral form, reportedly contain actinides, although no boron has been reported in them [22, 29]. The stable occurrence of the latter element in the nuclear waste crystals of zircon, apatite and fluorite is a favourable result considering the need for neutron poison-like boron in the neighbourhood of actinides to avoid potential nuclear criticality.

5. Conclusions

The waste forms composed of an assemblage of both minerals and glass offer greater potential for immobilizing chemically diverse waste streams that cannot be accommodated readily by crystalline or glass monoliths separately. The coexisting natural mineral and glass analogues contribute to the increase in the population and variety of compatible lattice sites, that are needed to accommodate the various ionic site specific elements. This contributes to increase in waste loading and durability. Both the growth of crystalline phases and waste form durability are dependent on the viscosity of the partial liquid that originates during HIPing. Although decreases in viscosity promote desirable crystal growths and eliminate formation of calcine relics, they aslo initiate the devitrification of glass into high surface area metastable phases during cooling in the HIP. This necessitates controlled addition of the viscosity modifier MgO to form durable basaltic microstructures with equilibrated crystals. The low leach rates of less than 1 g m^{-2} per day for all the elements, inclusive of the most mobile B, Cs and Na, result from the growth of stable crystalline phases and avoidance of glass devitrification. Increased durability for borosilicate glass matrix stems from the presence of high alumina. Although the waste loading in glass is of the order of 5 wt % compared with 95 wt % in crystals, the glass serves the purpose of bonding the heterogeneous microstructure, eliminating porosity and hosting the incompatible large ions like Cs. Compared to the ambient atmospheric process, HIP processing is environmentally safe. The entire processing occurs within the closed system of the canister. The surroundings of the HIP are free of contamination and no secondary wastes are produced during HIPing. With methodical design of the formulation in the light of fundamental crystallochemical and natural elemental distribution rules, the HIP process is suited for containing the volatile matter and for forming the desired phases by depression of the liquidus temperature under volatile pressure. The HIP process is in its infancy with regard to nuclear waste form development. But considering its practice in the industry for producing specialty materials and large scale products, the HIP process offers the potential for durably immobilizing the nuclear waste in large glass-crystal composite materials.

Acknowledgements

It is my pleasure to thank managers Dr D. A. Knecht, Mr J. H. Valentine and Dr J. A. Seydel for their encouragement of this work.

References

1. D. PINES, *Rev. Modern Phys.* **50** (1978) S1.
2. R. C. EWING and W. LUTZE, *Mater. Res. Soc. Bull.* **19** (1994) 16.
3. E. R. VANCE, *ibid.* **19** (1994) 28.
4. S. V. RAMAN, USDOE–WINCO 1173 (Westinghouse Idaho Nuclear Company, 1993).
5. L. L. HENCH, D. E. CLARK and J. CAMPBELL, *Nuclear Chem. Waste Management* **5** (1984) 149.
6. A. E. RINGWOOD, S. E. KESSON, N. G. WARE, W. HIBBERSON and A. MAJOR, *Nature* **278** (1979) 219.
7. H. W. LEVI, in "Scientific basis for nuclear waste management" edited by C. J. M. Northrup Jr (Plenum, New York, 1980). p. 21.
8. A. E. RINGWOOD, V. M. OVERSBY and W. SINCLAIR, *ibid.* p. 273.
9. A. E. RINGWOOD, S. E. KESSON and N. G. WARE, *ibid.* p. 265.
10. R. F. HAAKER and R. C. EWING, *ibid.* p. 281.
11. J. M. RUSIN, J. W. WALD and R. O. LOKKEN, *ibid.* p. 255.
12. A. B. HARKER, in "Radioactive waste forms for the future", edited by W. Lutze and R. C. Ewing (North-Holland, Amsterdam, 1988) p. 335.
13. A. B. HARKER and J. F. FLINTOFF, in "Scientific basis for nuclear waste management VII", edited by G.L. McVay (North-Holland, Amsterdam, 1984) p. 513.
14. G. J. McCARTHY, J. G. PEPIN, D. E. PFOERTSCH and D. R. CLARK, in "Symposium on ceramics in nuclear waste management", edited by T.D. Chikalla and J.E. Mendel (Technical Information Center, 1979) p. 315.
15. W. J. WEBER, R. C. EWING and W. LUTZE, in "Scientific basis for nuclear waste management XIX", edited by W. M. Murphy and D. A. Knecht, Materials Research Society Symposium Proceedings, Vol. 412 (Materials Research Society, Pittsburgh, PA 1996) p. 25.
16. B. E. BURAKOV, E. B. ANDERSON, V. S. ROVSHA, S. V. USHAKOV, R. C. EWING, W. LUTZE and W. J. WEBER, *ibid.* p. 33.
17. S. V. RAMAN, R. BOPP, T. A. BATCHELLER and Q. YAN, *ibid.* p. 133.
18. S. V. RAMAN, in "Glass as a waste form and vitrification technology: an internation workshop", (Board on Radioactive Waste Management, National Research Council, Washington, DC, 1996) p. 84.
19. G. B. MELLINGER and J. L. DANIEL, USDOE Report PNL–4955–1, (Pacific Northwest Laboratory, 1983).
20. C. M. JANTZEN, N. E. BIBLER, D. C. BEAM, C. L. CRAWFORD and M. A. PICKETT, USDOE Report WSRC–TR–93–181, (Westinghouse Savannah River Co., 1990).
21. J. R. FOWLER and M. J. PLODINEC, in Proceedings of the Third Annual International High Level Radioactive Waste Management (IHLRWM) Conference, Las Vegas, NV (1992) p. 904.
22. V. M. GOLDSCHMIDT, "Geochemistry" (Oxford University Press, 1958) p. 432.
23. S. V. RAMAN, in "Proceedings of Fifith Annual International High Level Radioactive Waste Management (IHLRW) Conference, Las Vegas, NV (1994) p. 1124.
24. S. V. RAMAN, in Proceedings of the Sixth Annual International High Level Radioactive Waste Management (IHLRWM) Conference, Las Vegas, NV (1995) p. 594.

25. MCC, "Nuclear waste materials handbook", (Materials Characterization Center, Hanford, WA), Report No. DOE/TIC-11400 (1983).
26. E. D. HESPE, *Atomic Energy Rev.* **9** (1971) 1.
27. I. S. E. CARMICHAEL, F. J. TURNER and J. VERHOOGEN, "Igneous petrology" (McGraw-Hill, New York, 1974) p. 739.
28. W. D. KINGERY, H. K. BOWEN and D. R. UHLMANN, "Introduction to ceramics" (Wiley, New York, 1976) p. 1032.
29. W. A. DEER, R. A. HOWIE and J. ZUSSMAN, "An introduction to the rock-forming minerals" (Longman, London, 1967) p. 528.

Received 7 August 1996
and accepted 8 July 1997